

# Understanding the Electrophoretic Deposition Accompanied by Electrochemical Reactions toward Structurally Colored Bilayer Films

Naoki Tarutani,<sup>†</sup> Ryo Uesugi,<sup>†</sup> Kensuke Uemura,<sup>†</sup> Kiyofumi Katagiri,<sup>\*,†</sup> Kei Inumaru,<sup>†</sup> and Yukikazu Takeoka<sup>‡</sup>

<sup>†</sup> Graduate School of Advanced Science and Engineering, Hiroshima University, Higashi-Hiroshima 739-8527, Japan

<sup>‡</sup> Graduate School of Engineering, Nagoya University, Nagoya 464-8603, Japan

\*Email: kktgr@hiroshima-u.ac.jp

**KEYWORDS:** *structurally colored coatings, colloidal amorphous arrays, chromaticity tuning, electrophoretic deposition; electrochemical reaction; bilayer films*

---

**ABSTRACT:** Safe, low-cost structurally colored materials are alternative colorants to toxic inorganic pigments and organic dyes. Colloidal amorphous arrays are promising structurally colored materials because of their angle-independent colors. In this study, we focused on precise tuning of the chromaticity by preparing bilayer colloidal amorphous arrays through electrophoretic deposition (EPD). Systematic investigations with various EPD conditions clarified the contributions of each condition to the EPD process and the competing electrochemical reactions, which enabled us to prepare well-colored coatings. EPD films composed of colloidal amorphous array bilayers were successfully synthesized with controlled film thickness. Chromaticity of the films was found to be precisely controlled by the EPD duration. We believe that this understanding of the EPD process and its application to synthesis of structurally colored bilayer films will bring structurally colored materials closer to practical industrial use.

---

## INTRODUCTION

Inorganic pigments and organic dyes are common materials for colorants in paints and printing inks, and for coloring plastics, ceramics, and metals. However, these common colorants have disadvantages. Inorganic pigments used on an industrial scale have included elements such as Cr, Cd, Hg, and Pb, which are harmful for human health and the environment,<sup>1-5</sup> and use of such elements is now strictly limited. Although synthetic organic dyes have been used on industrial scale because of their low cost and brighter colors compared with those produced by natural dyes, they are highly toxic and carcinogenic.<sup>6</sup> Therefore, much effort has been needed to remove such harmful substances from wastewaters; these processes can be expensive, slow and/or energy-intensive.<sup>7-9</sup> Structurally colored materials are novel alternatives to harmful inorganic pigments and organic dyes, and are expected to be applied in a wide range of fields<sup>10-13</sup>. The physical origin of the color of structurally colored materials is the interactions between visible light and sub-micrometer-scale fine structures.<sup>14</sup> The advantages of structurally colored materials are that the materials can be composed of safe and stable substances and the color will remain semipermanently unless the structures collapse. Assembly of monodispersed spherical particles is a versatile and reproducible way to prepare structurally colored materials showing desired colors.<sup>10,13,15,16</sup> Colloidal crystals (i.e.

ordered arrays of colloids) are a well-known and extensively investigated family of structurally colored materials. The color is controllable by tuning the diameter, refractive index, and ordering of particles.<sup>11,17</sup> Characteristically, the color of colloidal crystals depends on the viewing angle. Therefore, colloidal crystals have been used as color-sensing devices of pH/ionic strength,<sup>18</sup> solvent,<sup>19</sup> and mechanical stress,<sup>20</sup> but may not be appropriate for more practical situations, such as paint for traffic signs. Colloidal amorphous arrays are another type of structurally colored material, again composed of monodisperse particles. The difference is that colloidal amorphous arrays have only short-range order. Owing to this feature, colloidal amorphous arrays show angle-independent matt colors,<sup>21</sup> which should be suitable for a broader range of applications.

Colloidal amorphous arrays have been prepared through various methods, such as solvent evaporation,<sup>22</sup> a thermal-assisted process,<sup>23</sup> centrifugation technique,<sup>24</sup> drop-casting,<sup>25</sup> and spray-coating.<sup>26,27</sup> However, these processes make coating large surfaces quickly and/or treating complex-shaped materials difficult. Electrophoretic deposition (EPD) is a powerful, economical and energy-efficient technique that can be used to coat fine particles on large and complex surfaces as long as the surfaces are electrically conductive.<sup>28,29</sup> Our group has developed a method using EPD for synthesis of colloidal crystal/colloidal

amorphous array coatings.<sup>30–32</sup> Suspensions that contain monodisperse, spherical, SiO<sub>2</sub> particles were employed as starting materials. Films with controlled thickness were successfully prepared and show bright structural color, depending on the diameter of the deposited SiO<sub>2</sub> particles.<sup>30</sup> A recent study revealed that electrolytic co-deposition of Mg(OH)<sub>2</sub> allowed formation of colloidal amorphous arrays and significantly improved the mechanical robustness of the structurally colored films.<sup>32</sup> The EPD process accompanied by electrochemical Mg(OH)<sub>2</sub> formation is superior method to synthesize robust colloidal amorphous arrays.

Application as colorants requires chromaticity control of structurally colored materials. Chromaticity of colloidal crystals and colloidal amorphous arrays is known to depend on the diameter, refractive index, and ordering of particles.<sup>11,17,33</sup> Another approach to tune chromaticity is mixing prepared structural colored materials. Controlled colors have reportedly been achieved by mixing structurally colored materials through atomization deposition,<sup>34</sup> inkjet printing,<sup>35</sup> and an evaporation-based approach.<sup>36,37</sup> Here, in this study, we focused on the precise tuning of chromaticity of coating films composed of colloidal amorphous arrays prepared by an EPD process with accompanying electrochemical reactions. The EPD conditions were systematically changed to understand the kinetics and mechanism of the formation of colloidal amorphous array EPD films with co-deposited Mg(OH)<sub>2</sub> binder. Well-colored films with controllable thickness and colloidal amorphous array bilayer films were successfully prepared. The apparent color gradually changed as the upper layer formed on the lower layer of the synthesized bilayer structures. Chromaticity was found to linearly depend on the duration of EPD.

## EXPERIMENTAL PROCEDURE

**Materials.** Monodisperse spherical SiO<sub>2</sub> particles, with average diameters of 200, 240, 260, and 300 nm, were obtained from Fuji Chemical Co., Ltd. (Osaka, Japan). Iron oxide (Fe<sub>3</sub>O<sub>4</sub>) nanoparticles were provided by Toda Kogyo Corp. (Hiroshima, Japan). Magnesium nitrate hexahydrate (Mg(NO<sub>3</sub>)<sub>2</sub>·6H<sub>2</sub>O, ≥99.0%) was purchased from Kishida Chemical Co., Ltd. (Osaka, Japan). Ammonium hydroxide solution (NH<sub>4</sub>OH aq., 28 wt.%) and 2-propanol (≥99.7%) were obtained from Nacalai Tesque, Inc. (Kyoto, Japan). Hydrogen peroxide solution (H<sub>2</sub>O<sub>2</sub> aq., 30 wt.%) was purchased from Junsei Chemical Co., Ltd. (Tokyo, Japan). All reagents were used as received without further purification. Ultrapure water (resistivity 18.2 MΩ·cm) from a Millipore Milli-Q system (Merck Millipore, Billerica, MA, USA) was used in all experiments.

**Effects of SiO<sub>2</sub> Amount, Mg(NO<sub>3</sub>)<sub>2</sub> Amount, and Applied EPD Voltage on Formation of Colloidal Amorphous Array Films.** Different amounts (0.07–1.05 g) of SiO<sub>2</sub> particles (200 nm diameter) were dispersed by ultrasonication in 5 mL of cleaning solution (H<sub>2</sub>O:H<sub>2</sub>O<sub>2</sub> aq.:NH<sub>4</sub>OH aq., 5:1:1 by volume). The dispersion was heated at 60 °C for 30 min in a water bath to remove residual organic substances, and then centrifuged at 9390 g for 5 min. After removal of the supernatant, the sediments were redispersed in water. This centrifugation-redispersion process was repeated twice. Finally, SiO<sub>2</sub> particles were collected by centrifuged at 9390 g and redispersed in 2-

propanol (80 mL) by ultrasonication. Aqueous dispersion of Fe<sub>3</sub>O<sub>4</sub> nanoparticles (2.5 wt %, 0.6 mL) and different amounts of Mg(NO<sub>3</sub>)<sub>2</sub> aq. (3.5×10<sup>-2</sup> mol/L) (5–20 mL corresponding to 175–875 μmol of Mg(NO<sub>3</sub>)<sub>2</sub>) were added to the dispersion.

The EPD system used was the same as for our previous report.<sup>32</sup> Indium tin oxide (ITO)-coated glass substrates, size of 10 mm × 30 mm, were used as the working electrodes. The ITO-coated glass substrates were cleaned by the standard RCA-1 cleaning protocol, which was followed by rinsing with deionized water. Spiral shaped stainless-steel wires (SUS304) were used as the counter electrodes. The working and counter electrodes were immersed in the coating solutions. A specific voltage (5–40 V) was applied for a specific duration time using a direct current power supply (PAN110-3A, Kikusui Electronics Corp., Yokohama, Japan). After electrophoresis, the substrates were withdrawn from the solutions and dried at ambient temperature.

**Chromaticity Tuning by Preparation of Colloidal Amorphous Array Bilayer Films.** Dispersions of 0.7 g of SiO<sub>2</sub> particles (200, 240, 260, or 300 nm diameter) in 80 mL of 2-propanol were prepared via the cleaning procedure described above. Aqueous dispersion of Fe<sub>3</sub>O<sub>4</sub> nanoparticles (2.5 wt %, 0.6 mL) and Mg(NO<sub>3</sub>)<sub>2</sub> aq. (3.5×10<sup>-2</sup> mol/L, 5 mL) were added to the dispersions. ITO-coated glass pieces were immersed in the prepared solutions and EPD coated at an applied voltage of 20 V for 60 s to synthesize the lower layers of the bilayer films. These lower layer films were dried at room temperature and then immersed in a second solution containing different-sized SiO<sub>2</sub> particles. The upper layers of the bilayer films were formed on the lower layer films by electrophoresis at 20V for a certain time. Films were obtained after room temperature drying. The samples are denoted  $d_L$ - $d_U$ - $t$ , where  $d_L$  and  $d_U$  are SiO<sub>2</sub> particle diameters of lower and upper layers, respectively, and  $t$  is the duration (in seconds) of electrophoresis used to deposit the upper layer. Films with lower layers only were prepared using the same EPD conditions and used as control samples.

**Characterizations.** Optical images were taken using a digital camera to confirm the colors of the coatings. A field emission scanning microscope (SEM; S4800, Hitachi, Japan) was employed to characterize the ordering of the SiO<sub>2</sub> particles and the thickness of the EPD coating films. To observe the cross-sectional images, the coated substrates were cut using a diamond tip, 5 mm from the lower edge of each substrate. The reflectance spectra were collected with a UV–vis spectrometer (JASCO V-670) with an absolute reflectance measurement unit (ARMN-735).  $L^*a^*b^*$  color parameters of the products were evaluated following the CIE [Commission International de l'Eclairage] colorimetric method using a chromometer (CR-400, Konica Minolta, Inc., Tokyo, Japan) with illuminant C as light source and observer 2°. A chromometer was directly contacted with sample films for measurement. The parameter  $L^*$  is a measure of brightness (0 = black, 100 = white), and the  $a^*$  (red (+) to green (−) axis) and  $b^*$  (yellow (+) to blue (−) axis) parameters represent the color qualitatively. The color difference,  $\Delta E$ , was calculated as  $\Delta E = [(\Delta L^*)^2 + (\Delta a^*)^2 + (\Delta b^*)^2]^{1/2}$ . The chroma parameter ( $C$ ) expresses the color saturation of the product and can be calculated as:  $C = [(a^*)^2 + (b^*)^2]^{1/2}$ . The hue angle ( $h^\circ$ ) can be between 0° and 360°, and is within the following ranges for different colors: red, 350°–35°; orange, 35°–70°; yellow,

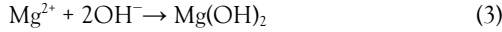
70°–105°; green, 105°–195°; blue, 195°–285°; and violet, 285°–350°. The value of  $h^\circ$  can be calculated as:  $h^\circ = \tan^{-1}(b^*/a^*)$ .

## RESULTS AND DISCUSSION

**Effects of SiO<sub>2</sub> Amount, Mg(NO<sub>3</sub>)<sub>2</sub> Amount, and Applied EPD Voltage on Formation of Colloidal Amorphous Array Films.** SiO<sub>2</sub> particles and Fe<sub>3</sub>O<sub>4</sub> particles have positively-charged surfaces arising from adsorbed Mg<sup>2+</sup> ions, and thus are electrophoretically deposited onto the ITO-coated glass substrate cathode.<sup>38–40</sup> The amount of electric charge passed,  $Q$ , during the deposition was used to characterize the process. Figure 1 shows the time-dependent increases in  $Q$  and film thickness. The  $Q$  linearly increased for the first ~1 min and became constant after 2 min. In this study,  $Q$  will increase due to the electrophoretic process and the following electrochemical reactions;<sup>41,42</sup>



The generated OH<sup>−</sup> will be consumed by the reaction:



and the Mg(OH)<sub>2</sub> formed will act to bind the deposited particles.<sup>43,44</sup> To clarify the contribution of each process to the  $Q$  value, a solution without SiO<sub>2</sub>/Fe<sub>3</sub>O<sub>4</sub> particles was employed. The  $Q$  showed same trend irrespective of the presence of SiO<sub>2</sub>/Fe<sub>3</sub>O<sub>4</sub> particles (Figure 1). This indicates that the major contribution to the  $Q$  value was electrochemical reactions. The coatings synthesized using the solution without SiO<sub>2</sub>/Fe<sub>3</sub>O<sub>4</sub> particles were dense films (Figure S1). The insulating Mg(OH)<sub>2</sub> layer formed on the substrate might suppress further electrochemical reactions, which would explain the  $Q$  value becoming constant. The  $Q$  values after 5 min duration were comparable between the two systems, which implies that the amounts of OH<sup>−</sup> generated and subsequent Mg(OH)<sub>2</sub> formed are comparable. The thicknesses of the EPD films were measured by cross-sectional SEM observation. The change of film thickness showed a similar trend to that of  $Q$  value—increasing linearly before becoming constant. The Mg(OH)<sub>2</sub> formed can be assumed to suppress EPD process as well. However, it has been reported that the thickness of EPD films tends to be constant even in systems without binder.<sup>45–47</sup> Further investigation is necessary to understand the kinetics and mechanism of the present EPD process.

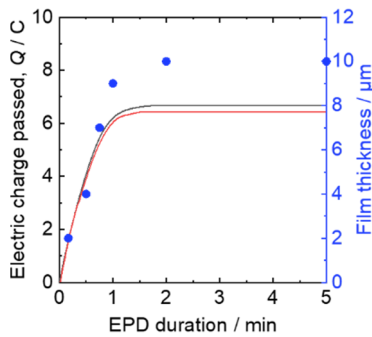


**Figure 1.** Duration-dependent increase of  $Q$  using starting solutions with (black solid line) and without (red dashed line) SiO<sub>2</sub>/Fe<sub>3</sub>O<sub>4</sub> particles. Blue points represent the thicknesses of films deposited using SiO<sub>2</sub>/Fe<sub>3</sub>O<sub>4</sub> particles dispersion. The inset optical image shows

the film for an EPD duration of 5 min. EPD conditions: 0.70 g SiO<sub>2</sub>, 525 μmol Mg(NO<sub>3</sub>)<sub>2</sub>, and applied voltage of 20 V.

The EPD kinetics are known to depend on the particles being deposited, the solution composition and the electrical conditions.<sup>28</sup> According to a previous report,<sup>48</sup> the deposited film weight,  $w$ , can be given as follows:

$$w = w_0(1 - e^{-kt}) \quad (4)$$

$$k = \frac{S}{V} \frac{\epsilon \zeta}{4\pi\eta} (E - \Delta E) \quad (5)$$

where  $w_0$  is initial weight of particles in the EPD solution,  $k$  is an apparent kinetic constant,  $t$  is duration,  $S$  is deposited area,  $V$  is the volume of EPD solution,  $\epsilon$  is the dielectric constant of EPD solution,  $\zeta$  is the zeta-potential of the particles,  $\eta$  is the viscosity of the EPD solution,  $E$  is the applied voltage, and  $\Delta E$  is the voltage drop across the deposited layer. In this study, the apparent density of the deposited films and the deposited area are assumed to be comparable among samples; therefore,  $w$  will be substituted by film thickness,  $\delta$ , with appropriate constant,  $A$ ;

$$\delta = Aw_0(1 - e^{-kt}) \quad (6)$$

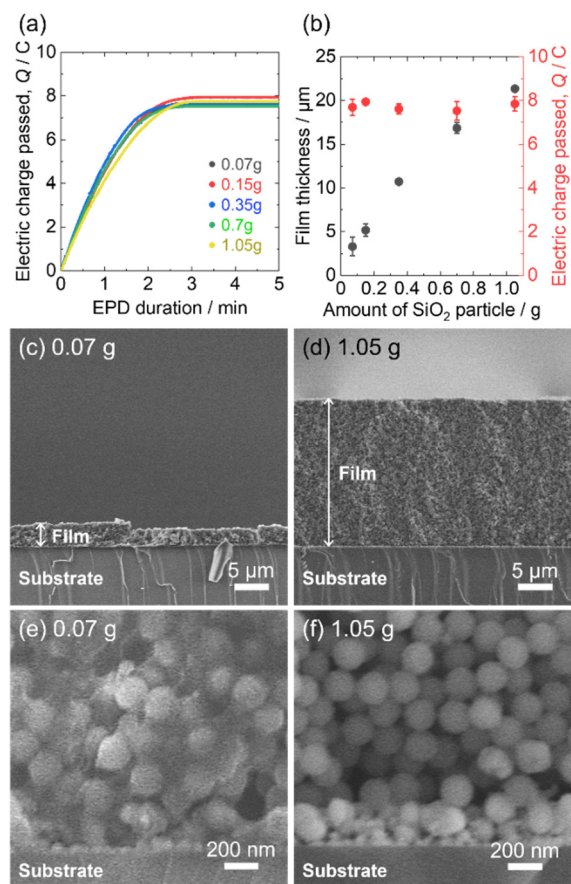
Considering this equation, the effects of SiO<sub>2</sub> particle amount, Mg(NO<sub>3</sub>)<sub>2</sub> amount, and applied voltage on the EPD process were investigated.

Figure 2a compares the duration-dependent  $Q$  values during EPD using solutions containing different amounts of SiO<sub>2</sub> particles. The rate of increase and the final value of  $Q$  were comparable for all systems, which again indicates that electrophoresis of SiO<sub>2</sub> particles only has minor effects on the  $Q$  value. The  $Q$  values after 5 min and the thickness of films formed were plotted (Figure 2b). Although  $Q$  values were almost constant, the thickness of EPD films linearly increased with SiO<sub>2</sub> amount, in agreement with equation (6). Increasing the amount of SiO<sub>2</sub> caused the number of electrophoresed particles per unit time to increase also. Films prepared from the solution containing 0.07 g SiO<sub>2</sub> showed rough surfaces (Figure 2c) and the interstices of the SiO<sub>2</sub> particles were filled with material (Figure 2e), which could be Mg(OH)<sub>2</sub>. In contrast, films prepared from the solution containing 1.05 g of SiO<sub>2</sub> showed smooth surfaces, with open spaces between the particles (Figure 2d and 2f). As is discussed above, the  $Q$  value is related to the amount of Mg(OH)<sub>2</sub> present. The total amounts of Mg(OH)<sub>2</sub> are therefore assumed to be comparable between these two systems, considering their similar  $Q$  values. Therefore, the proportion of Mg(OH)<sub>2</sub> in the obtained film was greater for the solution containing the smaller amount of SiO<sub>2</sub>, which led to the interstices between the SiO<sub>2</sub> particles being filled in. The films prepared with smaller amounts of SiO<sub>2</sub> in the starting solutions showed duller colors (Figure S2). It is deduced that the filling of the interstices by Mg(OH)<sub>2</sub> makes the refractive index contrast small, which in turns causes dulling of the color.

The effects of Mg(NO<sub>3</sub>)<sub>2</sub> amount and applied voltage on the electrophoretic behavior and electrochemical reactions were investigated. Figure 3a shows the duration-dependent change of  $Q$  value for solutions containing different amounts of Mg(NO<sub>3</sub>)<sub>2</sub>. Except for the 175 μmol Mg(NO<sub>3</sub>)<sub>2</sub> case,  $Q$  reached a constant value, which depended on amount of Mg(NO<sub>3</sub>)<sub>2</sub>. The  $Q$  value continuously increased, even after 30 min, when the starting solution contained 175 μmol of Mg(NO<sub>3</sub>)<sub>2</sub> (Figure S3a). The rate of increase of  $Q$  value, i.e., the electric current, in the initial 20 s,

increased with the amount of  $\text{Mg}(\text{NO}_3)_2$  (Figure 3c); this is caused by decreasing solution resistivity. The  $Q$  value at the plateau and the film thickness increased with increasing amount of  $\text{Mg}(\text{NO}_3)_2$  (Figure 3e). Considering these results and Figure 2a, the major factor dominating the  $Q$  value (that is the amount of  $\text{OH}^-$  generated) was the amount of  $\text{Mg}(\text{NO}_3)_2$  originally present. The generation rate of  $\text{OH}^-$  is known to be an important factor for the deposition process.<sup>49</sup> When the rate of generation of  $\text{OH}^-$  is sufficiently faster than the rate of consumption (in the present study, by the formation of  $\text{Mg}(\text{OH})_2$  of  $\text{OH}^-$ ,  $\text{OH}^-$  will diffuse from the surface of the electrode to the bulk solution. This will retard the covering of the electrode with insulating  $\text{Mg}(\text{OH})_2$ , and allow continuous deposition.

The applied voltage was varied from 5 V to 40 V.  $Q$  reached  $\sim 8$  C for applied voltages of 20, 30, and 40 V, but increased to  $\sim 10$  C and  $\sim 16$  C for applied voltages of 10 and 5 V, respectively; all curves displayed different initial slopes (Figure 3b and S3b). The average electric current over the initial 20 s increased with increasing applied voltage (Figure 3b and 3d), in an Ohmic manner. Considering equation (6) and a previous report<sup>47</sup>, the final  $Q$  values are expected to increase with applied voltage. However, the final  $Q$  values and film thicknesses were similar for applied voltages of 20, 30, and 40 V (Figure 3f). These results indicate that the voltage-dependence of the electrochemical  $\text{OH}^-$  generation rate was larger than that of the apparent electrophoretic kinetics, which led to suppression of the EPD process. Conditions that allow continuous film formation, faster deposition rate, and formation of well-colored films will be ideal to examine chromaticity control of colloidal amorphous array coating by EPD method. Therefore, a  $\text{SiO}_2$  amount of 0.7 g, an applied voltage of 20 V, and a  $\text{Mg}(\text{NO}_3)_2$  of amount of 175  $\mu\text{mol}$  were selected for subsequent experiments.



**Figure 2.** (a) Duration-dependent increase of  $Q$ , (b) film thickness (black) and  $Q$  value (red) after 5 min EPD; (c–f) SEM images of EPD films prepared with 175  $\mu\text{mol}$   $\text{Mg}(\text{NO}_3)_2$  and an EPD voltage of 20 V, (c),(d) cross-sectional SEM images of EPD films prepared using starting solutions containing 0.07 and 1.05 g of  $\text{SiO}_2$  particles, respectively, (e),(f) enlarged images of (c) and (d) near the substrates.

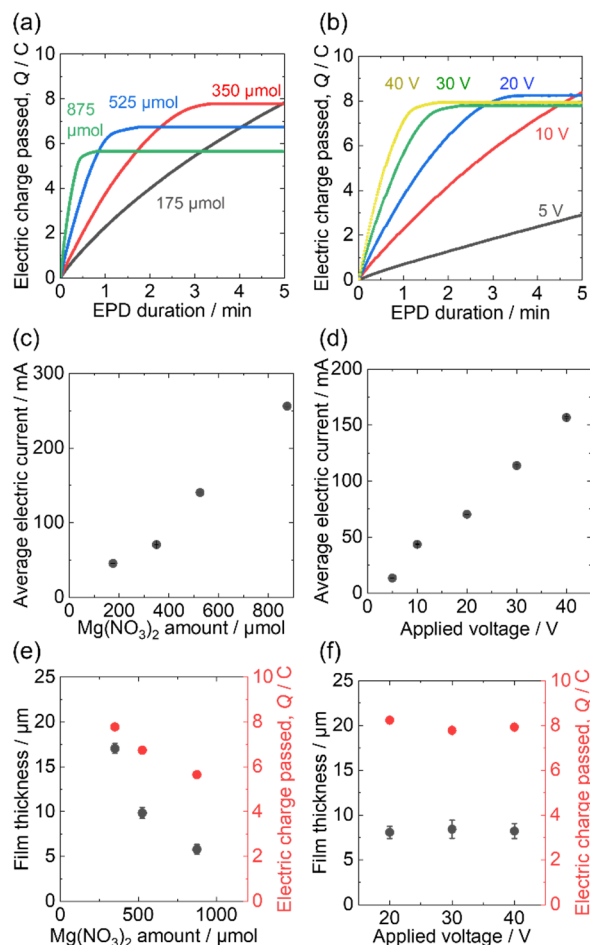


**Figure 3.** (a, b) Duration-dependent change of Q value; (c, d) average electric current during initial 20 s, and (e, f) film thickness (black) and Q value (red) after 5 min EPD, as different EPD parameters were varied: (a) (c) (e) varied  $\text{Mg}(\text{NO}_3)_2$  amount (constant 0.70 g  $\text{SiO}_2$  and 20 V applied voltage) and (b) (d) (f) varied applied voltage (constant 0.35 g  $\text{SiO}_2$  and 175  $\mu\text{mol}$   $\text{Mg}(\text{NO}_3)_2$ ).

### Synthesis and Color Evaluation of Structurally Colored Bilayer Films Composed of Colloidal Amorphous Arrays.

The particle-diameter dependence of the Q profile and thickness were investigated in advance (Figure S4). The trends for increase of Q value and thickness of the formed film were similar irrespective of particle diameter. The diameter of  $\text{SiO}_2$  particles was found to only have minor effects on both EPD kinetics and electrochemical reactions. Base samples with a lower layer array composed of 260 nm  $\text{SiO}_2$  particles were used to investigate the formation of bilayer structures and their effect on the chromaticity. Upper layers were deposited from a 200 nm  $\text{SiO}_2$  particle suspension using EPD durations of 10–420 s. The color of the film produced changed from green to blue green to blue (Figure 4a). Color change indicates formation of an upper layer containing 200 nm  $\text{SiO}_2$ . Figure 4b shows reflectance spectra of the synthesized films. The peak around  $\lambda = 550$  nm—corresponding to the structural color from the 260 nm particle arrays—decreased and the peak around  $\lambda = 430$  nm—corresponding to the structural color from 200 nm particle arrays—increased with EPD duration from 10–50 s. Cross-

sectional SEM images of 260-200-30 are shown in Figure 4c and 4d. There is a clear interface between the lower (260 nm particles) and upper (200 nm particles) layers. Takeoka *et al.* reported that the chromaticity of colloidal amorphous arrays depends on their thickness; color saturation decreased when the films became thicker than a threshold thickness.<sup>50</sup> Longer EPD durations were employed to elucidate the effect of thickness on the chromaticity of our bilayer films. Spectral changes became minor at EPD durations longer than 60 s, and were negligible over 300 s (Figure 5a). The thickness at 300 seconds is the threshold thickness where the light scattered by the lower layer cannot penetrate the thick upper layer. The threshold upper layer thickness was calculated as 19.2  $\mu\text{m}$  considering color difference,  $\Delta E$  (Figure 5b). The opposite bilayer structures 200-260-t ( $t = 0$ –480) were prepared to investigate the effect of particle diameter on the threshold upper layer thickness. The apparent color and reflectance spectra gradually changed with EPD duration (Figure S5a). The contribution of the structural color from the 200 nm particle array (around  $\lambda = 430$  nm) became negligible when the EPD duration was over 240 s (Figure S5b and S5c). Therefore, the threshold upper layer thickness was calculated as 18.7  $\mu\text{m}$  (Figure S5d), which is comparable to the thickness found for the 260-200-t system. This indicates that the effect of particle diameter on the light scattering was minor in this case and that the controllability of chromaticity is independent of the order in which the layers are deposited. For comparison, a film was prepared using a starting solution which contained both 200 nm and 260 nm  $\text{SiO}_2$  particles (Figure S6). These films showed a dull grayish color and a featureless linear reflectance spectrum. This is because of the lower degree of short-range ordering in the film with mixed particle sizes. In summary, colloidal amorphous array bilayers with controlled layer thickness enable the chromaticity of films to be tuned.

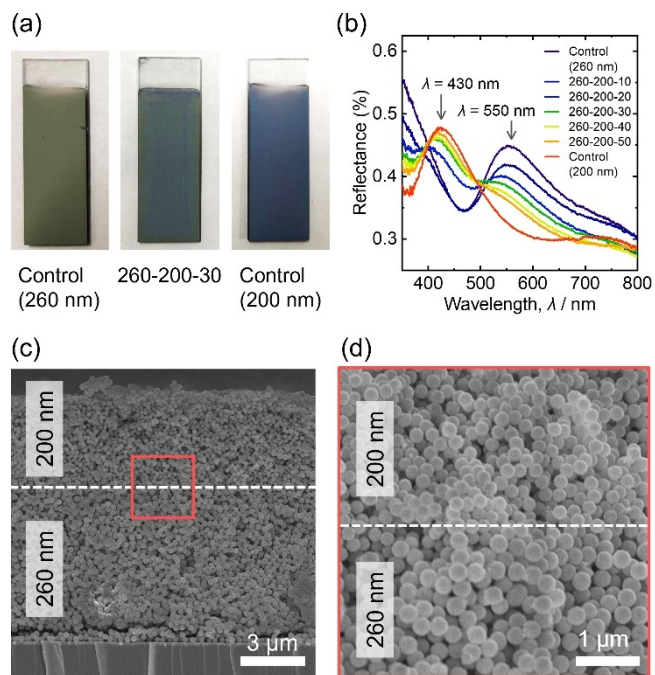


**Figure 4.** (a) Optical images of 260-200-30 and control samples. (b) Reflectance spectra of 260-200-t ( $t = 10$ –50) and control samples. (c) Cross-sectional SEM image of 260-200-30 and (d) enlargement of the area shown in the red square in (c).



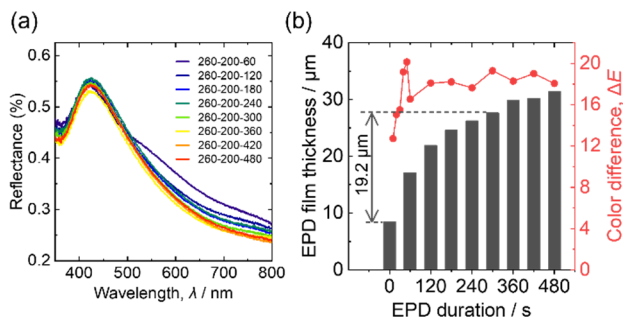


**Figure 5.** Effect of EPD duration on (a) reflectance spectra and (b) film thickness of (a) 260-200-*t* (*t* = 60–420, black to gray color) and (b) 260-200-*t* (*t* = 0–480) samples.

Bilayer films were prepared with different size combinations: 240-200-*t* and 300-200-*t*. Both systems showed gradual change of reflectance spectra and colors from light green to blue (240-200-*t*) and from red to blue (300-200-*t*), (Figure S7). The reflectance peaks assigned to arrays of SiO<sub>2</sub> particles of 240 nm ( $\lambda = 510$  nm) and 300 nm ( $\lambda = 640$  nm) decreased, and the peak derived from the 200 nm particle array increased, with increasing EPD duration. Both systems showed clear interfaces between their lower and upper layers (Figure S7e and S7f). Chromaticity change was evaluated using  $L^*a^*b^*$  and  $L^*C^*h^\circ$  color space (Table S1). Changing the particle diameter and duration time, enabled control of chromaticity. Both  $a^*$  and  $b^*$  were controlled over a range from positive to negative values (Figure 6a) and  $h^\circ$  values were from 137° to 327°, which indicates the that synthesized films cover a wide range of chromaticity. The values of  $a^*$  and  $b^*$  changed linearly with EPD duration for all the systems (Figure 6b and 6c). Therefore, the desired colorants can be obtained by precisely tuning the chromaticity through simply changing the EPD duration. In summary, chromaticity of colloidal amorphous array type structurally colored films can be controlled by preparing bilayer structures using EPD.

Structurally colored bilayer films composed of various sized SiO<sub>2</sub> particles were successfully prepared through EPD accompanied by electrochemical Mg(OH)<sub>2</sub> formation. This allows gradual chromaticity tuning of the films. Through the present approach, the structurally colored materials having a desired color will be easily coated on a large-area and/or complex-shaped conductive materials. In contrast, other methods, such as atomization deposition, inkjet printing, and an evaporation-based approach, will be beneficial for coating to non-conductive materials.

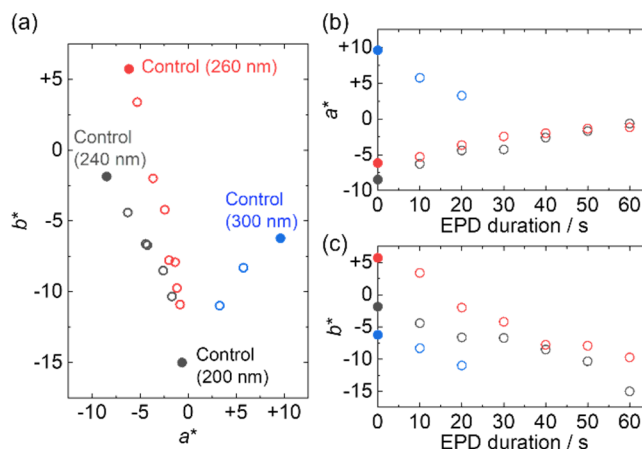


**Figure 6.** (a) Plot of color coordinates,  $a^*$  and  $b^*$ ; duration-dependent change of (b)  $a^*$  values and (c)  $b^*$  values of 240-200-*t* (*t* = 10–50) (black), 260-200-*t* (*t* = 10–120) (red), and 300-200-*t* (*t* = 30 and 60) (blue). Closed symbols represent control samples.

## CONCLUSIONS

In this study, chromaticity of structurally colored coatings composed of colloidal amorphous arrays was successfully tuned based on a detailed understanding of the EPD process. Investigations with various EPD conditions (amount of SiO<sub>2</sub> particles, amount of Mg salt, and applied EPD voltage) clarified the kinetics of the electrophoretic deposition of SiO<sub>2</sub> particles and electrochemical formation of Mg(OH)<sub>2</sub> binders. Conditions for preparation of well-colored coatings with controlled thickness over a wide range were found. Coating films composed of colloidal amorphous array bilayers, with SiO<sub>2</sub> particle diameter combinations of 200/260 nm, 260/200 nm, 200/240 nm, and 200/300 nm (lower/upper layer), were prepared with controlled upper-layer thickness. The threshold upper-layer thickness, above which the lower layer no longer affected the chromaticity of the film, was found to be approximately 19  $\mu$ m. Chromaticity of films was controlled with a range of  $a^*$  values from –8.49 to 9.61,  $b^*$  values from –15.01 to 5.74, and  $h^\circ$  values from 137° to 327° by varying the EPD duration. We believe that the facile approach to precise tuning of chromaticity presented in this study will bring structurally colored materials closer to practical use at an industrial scale.

## ASSOCIATED CONTENT

**Supporting Information.** SEM image of the film prepared using SiO<sub>2</sub>/Fe<sub>3</sub>O<sub>4</sub> absent solution. Optical images, time-dependent change of *Q* value, cumulative *Q* value, and film thickness of films prepared with different EPD conditions. Optical and SEM images, reflectance spectra, film thickness, and color coordinates of bilayer films.

## AUTHOR INFORMATION

Kiyofumi Katagiri – Graduate School of Advanced Science and Engineering, Hiroshima University, Higashi-Hiroshima 739-8527, Japan; orcid.org/0000-0002-9548-9835; Email: kktgr@hiroshima-u.ac.jp

## Authors

**Naoki Tarutani** – Graduate School of Advanced Science and Engineering, Hiroshima University, Higashi-Hiroshima 739-8527, Japan; orcid.org/0000-0003-0696-8082

**Ryo Uesugi** – Graduate School of Advanced Science and Engineering, Hiroshima University, Higashi-Hiroshima 739-8527, Japan

**Kensuke Uemura** – Graduate School of Advanced Science and Engineering, Hiroshima University, Higashi-Hiroshima 739-8527, Japan

**Kei Inumaru** – Graduate School of Advanced Science and Engineering, Hiroshima University, Higashi-Hiroshima 739-8527, Japan; orcid.org/0000-0001-6876-3854

**Yukikazu Takeoka** – Graduate School of Engineering, Nagoya University, Nagoya 464-8603, Japan; orcid.org/0000-0002-1406-0704

## ACKNOWLEDGMENTS

This work was supported by JSPS KAKENHI (Grant Numbers JP18K19132, JP19H04699, JP20H02439, JP20K15368, and JP21H00149). We thank Kate Nairn, PhD, from Edanz (<https://jp.edanz.com/ac>) for editing a draft of this manuscript.

## REFERENCES

- (1) Gilani, S. H.; Marano, M. Chromium Poisoning and Chick Embryogenesis. *Environ. Res.* **1979**, *19* (2), 427–431.
- (2) Singh, R.; Rustagi, N. Mercury and Health Care. *Indian J. Occup. Environ. Med.* **2010**, *14* (2), 45.
- (3) Rice, K. M.; Walker, E. M.; Wu, M.; Gillette, C.; Blough, E. R. Environmental Mercury and Its Toxic Effects. *J. Prev. Med. Public Heal.* **2014**, *47* (2), 74–83.
- (4) Turner, A. Cadmium Pigments in Consumer Products and Their Health Risks. *Sci. Total Environ.* **2019**, *657*, 1409–1418.
- (5) Wani, A. L.; Ara, A.; Usmani, J. A. Lead Toxicity: A Review. *Interdiscip. Toxicol.* **2015**, *8* (2), 55–64.
- (6) Vandevivere, P. C.; Bianchi, R.; Verstraete, W. Treatment and Reuse of Wastewater from the Textile Wet-Processing Industry: Review of Emerging Technologies. *J. Chem. Technol. Biotechnol.* **1998**, *72* (4), 289–302.
- (7) Fu, Y.; Viraraghavan, T. Fungal Decolorization of Dye Wastewaters: A Review. *Bioresour. Technol.* **2001**, *79* (3), 251–262.
- (8) Mohan, S. V.; Bhaskar, Y. V.; Karthikeyan, J. Biological Decolourisation of Simulated Azo Dye in Aqueous Phase by Algae *Spirogyra* Species. *Int. J. Environ. Pollut.* **2004**, *21* (3), 211–222.
- (9) Martínez-Huitle, C. A.; Brillas, E. Decontamination of Wastewaters Containing Synthetic Organic Dyes by Electrochemical Methods: A General Review. *Appl. Catal. B Environ.* **2009**, *87* (3–4), 105–145.
- (10) Takeoka, Y. Angle-Independent Structural Coloured Amorphous Arrays. *J. Mater. Chem.* **2012**, *22* (44), 23299–23309.
- (11) Zhao, Y.; Xie, Z.; Gu, H.; Zhu, C.; Gu, Z. Bio-Inspired Variable Structural Color Materials. *Chem. Soc. Rev.* **2012**, *41* (8), 3297–3317.
- (12) Dumanli, A. G.; Savin, T. Recent Advances in the Biomimicry of Structural Colours. *Chem. Soc. Rev.* **2016**, *45* (24), 6698–6724.
- (13) Kohri, M. Artificial Melanin Particles: New Building Blocks for Biomimetic Structural Coloration. *Polym. J.* **2019**, *51* (11), 1127–1135.
- (14) Kinoshita, S.; Yoshioka, S.; Miyazaki, J. Physics of Structural Colors. *Reports Prog. Phys.* **2008**, *71* (7), 076401.
- (15) Fudouzi, H.; Xia, Y. Colloidal Crystals with Tunable Colors and Their Use as Photonic Papers. *Langmuir* **2003**, *19* (23), 9653–9660.
- (16) Shang, G.; Maiwald, L.; Renner, H.; Jalas, D.; Dosta, M.; Heinrich, S.; Petrov, A.; Eich, M. Photonic Glass for High Contrast Structural Color. *Sci. Rep.* **2018**, *8* (1), 1–9.
- (17) Xia, Y.; Gates, B.; Yin, Y.; Lu, Y. Monodispersed Colloidal Spheres: Old Materials with New Applications. *Adv. Mater.* **2000**, *12* (10), 693–713.
- (18) Lee, K.; Asher, S. A. Photonic Crystal Chemical Sensors: PH and Ionic Strength. *J. Am. Chem. Soc.* **2000**, *122* (39), 9534–9537.
- (19) Ding, H.; Liu, C.; Ye, B.; Fu, F.; Wang, H.; Zhao, Y.; Gu, Z. Free-Standing Photonic Crystal Films with Gradient Structural Colors. *ACS Appl. Mater. Interfaces* **2016**, *8* (11), 6796–6801.
- (20) Wang, Y.; Shang, L.; Chen, G.; Sun, L.; Zhang, X.; Zhao, Y. Bioinspired Structural Color Patch with Anisotropic Surface Adhesion. *Sci. Adv.* **2020**, *6* (4), eaax8258.
- (21) Wang, S.; Liu, G.; Wang, L. Crystal Facet Engineering of Photoelectrodes for Photoelectrochemical Water Splitting. *Chem. Rev.* **2019**, *119* (8), 5192–5247.
- (22) Liu, T.; Vansaders, B.; Glotzer, S. C.; Solomon, M. J. Effect of Defective Microstructure and Film Thickness on the Reflective Structural Color of Self-Assembled Colloidal Crystals. *ACS Appl. Mater. Interfaces* **2020**, *12* (8), 9842–9850.
- (23) Yi, B.; Shen, H. Facile Fabrication of Crack-Free Photonic Crystals with Enhanced Color Contrast and Low Angle Dependence. *J. Mater. Chem. C* **2017**, *5* (32), 8194–8200.
- (24) Torres, L.; Margaronis, A.; Bellato Meinhardt, B. M.; Granzow, L.; Ayyub, O. B.; Kofinas, P. Rapid and Tunable Method to Fabricate Angle-Independent and Transferable Structurally Colored Films. *Langmuir* **2020**, *36* (5), 1252–1257.
- (25) Ge, D.; Yang, X.; Chen, Z.; Yang, L.; Wu, G.; Xia, Y.; Yang, S. Colloidal Inks from Bumpy Colloidal Nanoparticles for the Assembly of Ultrasmooth and Uniform Structural Colors. *Nanoscale* **2017**, *9* (44), 17357–17363.
- (26) Takeoka, Y.; Yoshioka, S.; Takano, A.; Arai, S.; Nueangnoraj, K.; Nishihara, H.; Teshima, M.; Ohtsuka, Y.; Seki, T. Production of Colored Pigments with Amorphous Arrays of Black and White Colloidal Particles. *Angew. Chemie - Int. Ed.* **2013**, *52* (28), 7261–7265.
- (27) Kohri, M.; Nannichi, Y.; Taniguchi, T.; Kishikawa, K. Biomimetic Non-Iridescent Structural Color Materials from Polydopamine Black Particles That Mimic Melanin Granules. *J. Mater. Chem. C* **2015**, *3* (4), 720–724.
- (28) Ferrari, B.; Moreno, R. EPD Kinetics: A Review. *J. Eur. Ceram. Soc.* **2010**, *30* (5), 1069–1078.
- (29) Corni, I.; Ryan, M. P.; Boccacini, A. R. Electrophoretic Deposition: From Traditional Ceramics to Nanotechnology. *J. Eur. Ceram. Soc.* **2008**, *28* (7), 1353–1367.
- (30) Katagiri, K.; Tanaka, Y.; Uemura, K.; Inumaru, K.; Seki, T.; Takeoka, Y. Structural Color Coating Films Composed of an Amorphous Array of Colloidal Particles via Electrophoretic Deposition. *NPG Asia Mater.* **2017**, *9* (3), e355.
- (31) Katagiri, K.; Uemura, K.; Uesugi, R.; Inumaru, K.; Seki, T.; Takeoka, Y. Structurally Colored Coating Films with Tunable Iridescent Fabricated: Via Cathodic Electrophoretic Deposition of Silica Particles. *RSC Adv.* **2018**, *8* (20), 10776–10784.
- (32) Katagiri, K.; Uemura, K.; Uesugi, R.; Tarutani, N.; Inumaru, K.; Uchikoshi, T.; Seki, T.; Takeoka, Y. Robust Structurally Colored Coatings Composed of Colloidal Arrays Prepared by the Cathodic Electrophoretic Deposition Method with Metal Cation Additives. *ACS Appl. Mater. Interfaces* **2020**, *12* (36), 40768–40777.
- (33) Ding, H.; Liu, C.; Gu, H.; Zhao, Y.; Wang, B.; Gu, Z. Responsive Colloidal Crystal for Spectrometer Grating. *ACS Photonics* **2014**, *1* (2), 121–126.
- (34) Li, Q.; Zhang, Y.; Shi, L.; Qiu, H.; Zhang, S.; Qi, N.; Hu, J.; Yuan, W.; Zhang, X.; Zhang, K. Q. Additive Mixing and Conformal Coating of Noniridescent Structural Colors with Robust Mechanical Properties Fabricated by Atomization Deposition. *ACS Nano* **2018**, *12* (4), 3095–3102.
- (35) Bai, L.; Mai, V. C.; Lim, Y.; Hou, S.; Möhwald, H.; Duan, H. Large-Scale Noniridescent Structural Color Printing Enabled by

- Infiltration-Driven Nonequilibrium Colloidal Assembly. *Adv. Mater.* **2018**, 30 (9), 1–7.
- (36) Yan, Q.; Teh, L. K.; Shao, Q.; Wong, C. C.; Chiang, Y. M. Layer Transfer Approach to Opaline Hetero Photonic Crystals. *Langmuir* **2008**, 24 (5), 1796–1800.
- (37) Sakai, M.; Kim, H.; Arai, Y.; Teratani, T.; Kawai, Y.; Kuwahara, Y.; Abe, K.; Kuwana, Y.; Ikeda, K.; Yamada, K.; Takeoka, Y. Monodisperse Silica Nanoparticle-Carbon Black Composite Microspheres as Photonic Pigments. *ACS Appl. Nano Mater.* **2020**, 3 (7), 7047–7056.
- (38) Pashley, R. M.; Israelachvili, J. N. Dlv and Hydration Forces between Mica Surfaces in  $Mg^{2+}$ ,  $Ca^{2+}$ ,  $Sr^{2+}$ , and  $Ba^{2+}$  Chloride Solutions. *J. Colloid Interface Sci.* **1984**, 97 (2), 446–455.
- (39) Zohar, O.; Leizeron, I.; Sivan, U. Short Range Attraction between Two Similarly Charged Silica Surfaces. *Phys. Rev. Lett.* **2006**, 96 (17), 1–4.
- (40) Ruiz-Cabello, F. J. M.; Trefalt, G.; Csendes, Z.; Sinha, P.; Oncsik, T.; Szilagyi, I.; Maroni, P.; Borkovec, M. Predicting Aggregation Rates of Colloidal Particles from Direct Force Measurements. *J. Phys. Chem. B* **2013**, 117 (39), 11853–11862.
- (41) Matsumoto, Y.; Morikawa, T.; Adachi, H.; Hombo, J. A New Preparation Method of Barium Titanate Perovskite Film Using Electrochemical Reduction. *Mater. Res. Bull.* **1992**, 27 (11), 1319–1327.
- (42) Gal - Or, L.; Silberman, I.; Chaim, R. Electrolytic  $ZrO_2$  Coatings. I. Electrochemical Aspects. *J. Electrochem. Soc.* **1991**, 138 (7), 1939–1942.
- (43) Siracuse, J. A.; Talbot, J. B.; Sluzky, E.; Hesse, K. R. The Adhesive Agent in Cataphoretically Coated Phosphor Screens. *J. Electrochem. Soc.* **1990**, 137 (1), 346–348.
- (44) Russ, B. E.; Talbot, J. B. An Analysis of the Binder Formation in Electrophoretic Deposition. *J. Electrochem. Soc.* **1998**, 145 (4), 1253–1256.
- (45) Zhitomirsky, I.; Gal-Or, L. Electrophoretic Deposition of Hydroxyapatite. *J. Mater. Sci. Mater. Med.* **1997**, 8 (4), 213–219.
- (46) Zhang, J.; Lee, B.  $BaTiO_3$  Based X7R Dielectric Thick Films. *J. Am. Ceram. Soc.* **2000**, 83 (10), 2417–2422.
- (47) Wang, Y. C.; Leu, I. C.; Hon, M. H. Kinetics of Electrophoretic Deposition for Nanocrystalline Zinc Oxide Coatings. *J. Am. Ceram. Soc.* **2004**, 87 (1), 84–88.
- (48) Zhang, Z.; Huang, Y.; Jiang, Z. Electrophoretic Deposition Forming of  $SiC$  -  $TZP$  Composites in a Nonaqueous Sol Media. *J. Am. Ceram. Soc.* **1994**, 77 (7), 1946–1949.
- (49) Zhitomirsky, I. Cathodic Electrodeposition of Ceramic and Organoceramic Materials. Fundamental Aspects. *Advances in Colloid and Interface Science*. 2002, pp 279–317.
- (50) Iwata, M.; Teshima, M.; Seki, T.; Yoshioka, S.; Takeoka, Y. Bio-Inspired Bright Structurally Colored Colloidal Amorphous Array Enhanced by Controlling Thickness and Black Background. *Adv. Mater.* **2017**, 29 (26), 1–8.



## TABLE OF CONTENTS GRAPHIC

